SCIENCE CHINA
Technological Sciences

• Article •

August 2015 Vol.58 No.8: 1299–1317
doi: 10.1007/s11431-015-5853-9

Three-layer intelligence of planetary exploration wheeled mobile robots: Robint, virtint, and humint

DING Liang[1*], GAO HaiBo[1*], DENG ZongQuan[1], LI YuanKai[2], LIU GuangJun[3], YANG HuaiGuang[1] & YU HaiTao[3*]

[1] *State Key Laboratory of Robotics and System, Harbin Institute of Technology, Harbin 150001, China;*
[2] *School of Aeronautics and Astronautics, University of Electronic Science and Technology of China, Chengdu 611731, China;*
[3] *Department of Aerospace Engineering, Ryerson University, Toronto M5B 2K3, Canada*

Received February 5, 2015; accepted May 20, 2015; published online June 16, 2015

The great success of the Sojourner rover in the Mars Pathfinder mission set off a global upsurge of planetary exploration with autonomous wheeled mobile robots (WMRs), or rovers. Planetary WMRs are among the most intelligent space systems that combine robotic intelligence (robint), virtual intelligence (virtint), and human intelligence (humint) synergetically. This article extends the architecture of the three-layer intelligence stemming from successful Mars rovers and related technologies in order to support the R&D of future tele-operated robotic systems. Double-layer human-machine interfaces are suggested to support the integration of humint from scientists and engineers through supervisory (Mars rovers) or three-dimensional (3D) predictive direct tele-operation (lunar rovers). The concept of multilevel autonomy to realize robint, in particular, the Coupled-Layer Architecture for Robotic Autonomy developed for Mars rovers, is introduced. The challenging issues of intelligent perception (proprioception and exteroception), navigation, and motion control of rovers are discussed, where the terrains' mechanical properties and wheel-terrain interaction mechanics are considered to be key. Double-level virtual simulation architecture to realize virtint is proposed. Key technologies of virtint are summarized: virtual planetary terrain modeling, virtual intelligent rover, and wheel-terrain interaction mechanics. This generalized three-layer intelligence framework is also applicable to other systems that require human intervention, such as space robotic arms, robonauts, unmanned deep-sea vehicles, and rescue robots, particularly when there is considerable time delay.

planetary exploration rovers, robot intelligence, virtual intelligence, three-layer architecture

Citation: Ding L, Gao H B, Deng Z Q, et al. Three-layer intelligence of planetary exploration wheeled mobile robots: Robint, virtint, and humint. Sci China Tech Sci, 2015, 58: 1299–1317, doi: 10.1007/s11431-015-5853-9

1 Introduction

Exploration of planets such as Mars and the Moon with autonomous wheeled mobile robots (WMRs), or rovers, has already been shown to be effective by the successfully executed rover-based missions. In the 1970s, the former USSR launched two eight-wheeled rovers called "Lunakhod-1" and "Lunakhod-2", which were directly tele-operated by operators on the Earth [1]. The achievement of the Sojourner rover of the Mars Pathfinder exploration mission [2] in 1997 began a worldwide upsurge in the exploration of planets with autonomous WMRs. In 2003, the Mars exploration rovers (MERs) Spirit and Opportunity were launched [3], and have undergone many years of activity on Mars and made many significant discoveries [4,5]. On August 6, 2012, NASA's Mars Science Laboratory (MSL) spacecraft successfully landed on Aeolis Palus in Gale Crater, and the

*Corresponding authors (email: liangding@hit.edu.cn, gaohaibo@hit.edu.cn, yukings1984@126.com)

Curiosity rover [6] started its exploration on the red planet. Several other rover-based planetary exploration missions are currently in progress. As the first mission in ESA's Aurora Exploration Programme, ExoMars was scheduled to launch in 2013 and is now delayed to 2018; it will carry a rover with several scientific instruments dedicated to exobiology and geology research [7]. China's six-wheeled Yutu (Jade Rabbit) rover of Chang'e-3 mission has reached the surface of the Moon on December 14, 2013 [8]. The SELENE-2 mission of Japan has been planned to land on the Moon and investigate its surface, rocks, and subsurface using a lunar lander and a rover [9].

According to NASA's Solar System exploration roadmap, "habitability," the guiding theme of planetary exploration missions is decomposed into five related science objectives [10]: The origin of the Sun's family of planets, the Solar System's evolution, life's origins, extraterrestrial life, and hazards and resources that affect humans in space. Planetary rovers are expected to help scientists achieve such objectives by performing remote experiments on the soil, rocks, atmosphere, etc. at various locations [11,12].

To carry out in-situ experiments and realize complex scientific goals on planetary surfaces that are a long distance from the Earth, planetary rovers have been among the most intelligent space systems [13–15]. Their robotic intelligence is implemented by the development of software that supports the autonomous capabilities of navigation and mobility control, scientific instrument placement onto surface samples, onboard resource management, science data gathering, etc. [13]. Rovers are expected to be increasingly intelligent in order to satisfy the requirements of more challenging missions in complex unknown terrains.

However, current robotic intelligence cannot ensure that planetary rovers can fulfill the complicated mission tasks autonomously with little intervention from scientists and engineers. Tele-operation—the manipulation of a robot that allows an operator to perform tasks at a distance in a hostile environment where human access is difficult but human intelligence is necessary—is a good way to combine the intelligence and maneuverability of humans with the capacity of robots [16]. Scientists must select targets or destination points according to results downlinked from rovers, such as images and terrain characteristics [17], and the operators drive the rovers by selecting the waypoints and generating command sequences to guide the rover to realize its objectives [18]. In particular, if the rovers encounter problems that they cannot manage themselves, engineers must use their intelligence and experience to aid them. For instance, in 2005, Opportunity became stuck in the soft Purgatory Dune, and operators spent around five weeks attempting to rescue it through planning, testing, and carefully monitored driving based on ground experiments and simulations [19]. To support effective integration of human intelligence from scientists and engineers into planetary exploration missions, there must be efficient human-machine interfaces (HMIs) of hardware and software. For instance, the Web Interface for Telescience [17] is an Internet-based tool that enables members of geographically distributed science teams to participate in mission planning for planetary rovers, and Rover Sequencing and Visualization Program (RSVP) [18] tools are used by engineers to process and visualize terrain, and to generate and validate command sequences for rovers.

Because of the long distance and bandwidth limitations, the time delay of transmission from the Earth to the Moon is approximately several seconds, which makes the direct tele-operation of lunar rovers unstable. Virtual simulation-based 3D predictive display could be used to realize successive tele-operation of lunar rovers [20]. The round-trip time delay between the Earth and Mars ranges from approximately 20 to 40 min depending on the relative positions of the planets [21]; thus, supervisory tele-operation is used for Mars rovers to update mission planning every day after command sequence validation based on virtual simulation. Both successive tele-operation mode based on 3D display and supervisory tele-operation mode with command validation require the support of virtual simulation. Virtual intelligence is crucial to implementing high-fidelity simulation by combining the intelligent exploration rover, rough and deformable planetary terrain, and rover-terrain interaction.

Therefore, planetary rovers have a three-layer intelligence architecture—human intelligence (humint), robotic intelligence (robint), and virtual intelligence (virtint)—and the majority of humint and virtint can be integrated into rovers with continuous improvement of robint in order to develop autonomous exploration rovers with little or no need for intervention from scientists and engineers. The contribution of this paper lies in extending the general concept of the three-layer intelligence architecture stemming from planetary exploration rovers to the application of other space systems and tele-operated robots, and in providing an overview , including future prospects, of the technologies of robint, humint, and virtint for planetary exploration rovers.

The remainder of this paper is organized as follows. Section 2 advances the three-layer intelligence architecture of planetary rovers. Section 3 describes humint, which includes the intelligence of scientists and engineers, and HMIs. Section 4 summarizes the prospects for robotic intelligence, including framework, perception, navigation, and motion control. Section 5 discusses the virtual intelligence framework and key technologies. Finally, concluding remarks are drawn in Section 6.

2 Three-layer architecture of planetary exploration rovers' intelligence

In this section, we analyze the requirements of missions involving Mars rovers and lunar rovers according to their scientific goals and discuss the intelligence that is required

for a tele-operated rover system. A three-layer intelligence architecture for the rovers is designed to support the implementation of planetary exploration rovers.

2.1 Mission requirement analysis

Planetary rovers achieve mission objectives through carrying out various scientific experiments using their onboard instruments. The objective of Mars exploration concentrates on searching for extraterrestrial life because Mars is considered as one of the most likely places. The primary objective of the Spirit and Opportunity rovers is to search for evidence of past water at Gusev Crater and Meridiani Planum on the opposite sides of Mars by studying the rocks and soils at various places [22]. The MSL mission with the Curiosity rover (Figure 1) attempts to determine whether life ever arose on Mars, characterize the Martian climate and geology, and study the planet's habitability for future human exploration, using an overall science strategy of "following the water" [25]. ESA's ExoMars rover will also attempt to search for signs of past and present life on Mars and to characterize the water and geochemical environment as a function of depth to within 2 m from the subsurface [26]. Unlike Mars, the Moon is considered to be a cornerstone for planetary science and ideal future habitat [27]. It started its evolution in the same form as the Earth and other planets, and underwent limited weathering processes because it has no atmosphere and has been exposed to solar wind; thus the Moon provides a record of the Sun's evolution, planetary differentiation, and early evolution. Moreover, living habitats and refueling stations for humans could be established on the Moon because it contains the ingredients for fuels and supporting life, and it takes only several days to arrive at the Moon [27]. The mission goals of the SELENE-2 lunar exploration, which has a lander and a mobility system, are to investigate radial variations of structure and chemical composition and to perform astronomical observations of the unique lunar environment with a view to future lunar utilization [28]. China's Change'e-3 mission has investigated the topography and geomorphology of the lunar surface, comprehensive utilization of lunar soil, lunar dynamics, and space weather with a six-wheeled lunar rover, an experimental mockup of which is shown in Figure 2.

Most planetary rovers have six independently driven wheels (the four corner wheels have steering motors) and rocker-bogie suspensions with passive joints, which give them high traversability on rough terrain; they also carry a number of sensors and cameras for autonomous navigation and perception of both the environment and their own status. They have a comprehensive suite of instruments dedicated to in-situ observation and investigation with the help of robotic arms. For example, each of the Spirit and Opportunity rovers have a five-degrees-of-freedom arm called the Instrument Deployment Device [30], four sets of stereoscopic cameras, three spectrometers, a Microscopic Imager, and a Rock Abrasion Tool for cleaning and grinding rock surfaces [31]. Figure 3 shows the location of scientific instruments on the Curiosity rover [32]. The instruments can be divided

Figure 1 Curiosity rover at Gale Crater [23]. Curiosity has a mass of 899 kg with 80 kg of scientific instruments; it is 2.9 m in length, 2.7 m in width, and 2.2 m in height [24].

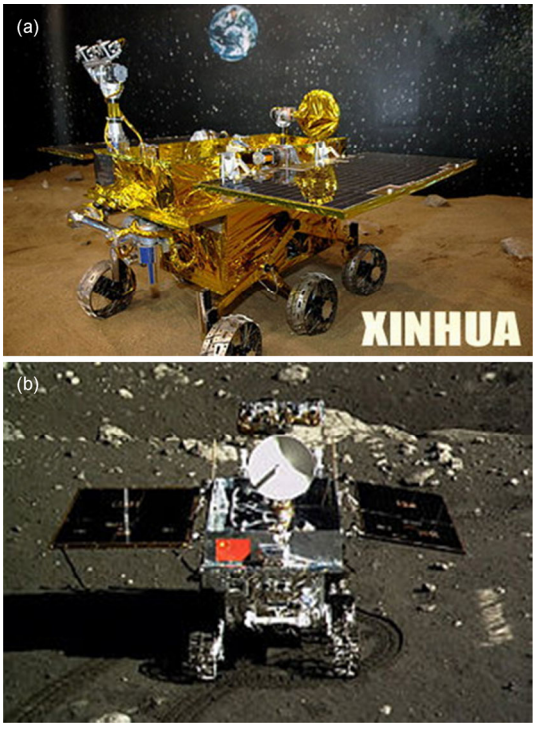

Figure 2 Lunar rovers of China. (a) Mockup of Yutu rover of China's Chang'e-3 mission, taken by Wenjie Zhou of Xinhua News Agency, China, on October 31, 2006, when the rover was exhibited at the Zhuhai Airshow [29]. The rover was assembled by the Chinese Academy of Space Technology, and the locomotion system was researched and developed by the authors in State Key Laboratory of Robotics and System, Harbin Institute of Technology. (b) Yutu rover on the lunar surface, photographed by the Chang'e-3 lander [8].

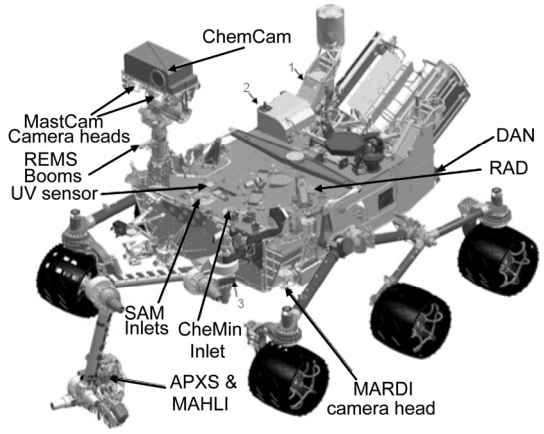

Figure 3 Scientific instruments of the Curiosity rover and their locations [32].

into four categories: (1) The remote sensing instruments located on the remote sensing mast—MastCam (Mast Camera) and ChemCam (Chemistry and Camera complex); (2) the contact scientific instruments at the end of the robotic arm— APXS (Alpha Particle X-ray Spectrometer) and MAHLI (Mars Hand Lens Imager); (3) the analytical laboratory instruments inside the rover body—CheMin (Chemistry and Mineralogy) and SAM (Sample Analysis at Mars); and (4) the environmental instruments—RAD (Radiation Assessment Detector), DAN (Dynamic Albedo of Neutrons), REMS (Rover Environmental Monitoring Station), and MARDI (Mars Descent Imager). There is also a Sample Acquisition, Processing, and Handling subsystem used for the acquisition of rock and soil samples and the processing of samples into fine particles, which are then distributed to the scientific instruments. The Sample Acquisition, Processing, and Handling subsystem consists of a robotic arm on the end of which are turret-mounted devices, which include a drill, brush, soil scoop, sample processing device, and mechanical and electrical interfaces to the two contact scientific instruments.

Planetary rovers must primarily face two types of challenges. The first is how to traverse complex and unknown terrains safely to search for features of interest; the second is how to carry out scientific investigation step by step by combined usage of various types of tools and instruments. Tackling such challenges requires long-term efforts to develop autonomous robotics systems that integrate the intelligence of the experienced scientists and engineers, such as selection of targets of interest, onboard evaluation of the scientific value of local targets, and the interaction of instruments [18]. In the meantime, it is essential to have autonomous path planning and traversability evaluation while taking into account the mechanical property of terrains and avoiding wheel stuck autonomously. However, two obstacles hinder the realization of such complete intelligent planetary rovers: one is the limitations of technology because there remain many issues yet to be resolved; the other is that the planetary rovers have extremely limited computational and storage resources because of high radiation levels, large temperature changes, and low power in space. The Sojourner rover has a 0.1 MHz Intel 80C85 CPU with 512 kB RAM and 176 kB flash memory; each MER rover has a single general purpose processor, 20 MHz RAD6000 CPU with 128 MB RAM and 256 MB flash memory; and the MSL rover has a 200 MHz RAD750 PowerPC with 256 MB RAM and 512 MB flash memory [14,15]. The rovers run many parallel tasks simultaneously using the VxWorks operating system, leaving less than 75% of the CPU time available for autonomous software.

To overcome the current obstacles to carrying out challenging missions, the tele-operation approach could be used to compensate for the limited robotic intelligence and the limited onboard calculation resources by means of humint and virtint, respectively.

2.2 Three-layer intelligence architecture

The three-layer intelligence architecture of planetary rovers is illustrated in Figure 4 and comprises a robint layer, a humint layer, and a virtint layer.

The robotic intelligence layer corresponds to the rover's autonomy, including autonomous perception (such as proprioception of the rover's status and its interaction with the terrain, exteroception of the terrain's geometry and mechanical properties), navigation, and motion control, the best-known example of which is Coupled-Layer Architecture for Robotic Autonomy (CLARAty) [33,34] developed by NASA/JPL. Robint is the most important intelligence in the success of exploration missions, particularly for supervisory tele-operated rovers such as the Mars rovers, and they are continuously developed by integrating more and more humint and virtint. The human intelligence layer compromises HMIs in the form of software and hardware for scientists and engineers. The web-based interface (for instance, Web Interface for Telescience [17]) allows geographically distributed scientists to participate in the mission planning of rovers that are far from the control center. Software capable of rover data analysis and command sequence generation (for instance, RSVP [18,35]) is used by engineers to analyze the downlinked information on the rover and the environment, generate and validate command sequences according to scientists' suggestions, and uplink them to the rovers. The virtual intelligence layer comprises an intelligent virtual rover and a virtual environment capable of simulating the motion of planetary rovers for command sequence validation; examples include the ROver Analysis, Modeling, and Simulation (ROAMS) software [36]. Low-level simulation could be executed kinematically and swiftly for scientists to estimate the mission's feasibility, whereas high-fidelity simulation is executed while considering kinematics, dynamics, and in particular wheel-terrain interaction mechanics, with which engineers and scientists

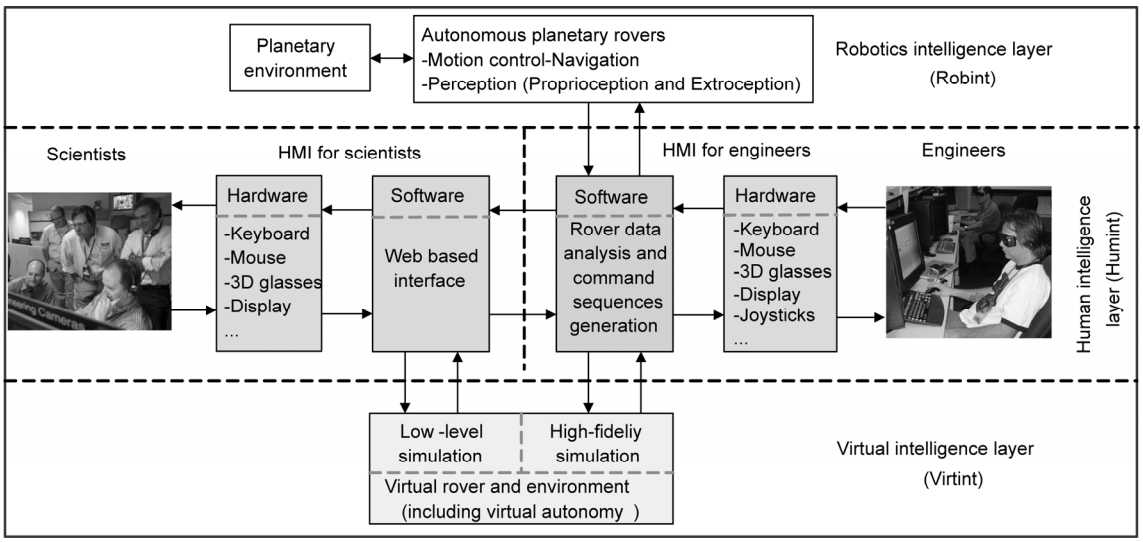

Figure 4 Three-layer intelligence architecture for planetary rovers.

at the control center could validate the motion of rovers before commands are uplinked. Robotic intelligence programs should be integrated into the simulation software with minor adjustments for adaptation to the difference between the actual rover and the environment and the virtual counterparts.

During the development of Mars rovers, JPL developed various software to realize the three-layer intelligence of planetary rovers. Around ten years before the launch of Curiosity rover, the Mars Technology Program, in conjunction with the MSL mission, funded three complementary infrastructure elements—ROAMS, Web Interface for Telescience, and CLARAty [37]—which respectively correspond to each layer of the three-layer intelligence architecture.

3 Humint: Integrating intelligence of scientists and engineers through HMIs

In designing a rover, scientists set its requirements such as payload and mobility according to the scientific goals, and the engineers develop the rover to satisfy these requirements. During the operational phase, the science team plans the rover missions in collaboration with the engineering team, who will in turn generate command sequences to control the rovers after validation with a simulation platform. The HMIs that help to integrate the intelligence of scientists and operators into the rovers are important during the operational phase.

3.1 Intelligence of scientists for planetary rovers

Scientists play important roles during the operational phase of planetary rovers while executing exploration missions in at least two aspects.

(1) Science team members tell the rover "what to do" by producing an acceptable science plan and marking targets of interest in local terrain based on the scientific goals and the suggestions of engineering team members. Figure 5 shows the missions planned for the Sojourner rover [38]. Scientists obtained fruitful scientific findings as expected by analyzing the experimental results downlinked from the rovers while performing the scientific missions. For example, using experimental data such as spectra obtained by Spirit's Miniature Thermal Emission Spectrometer (Mini-TES) at eight locations on the Comanche outcrops, Richard et al. identified outcrops rich in magnesium-iron carbonate in the Columbia Hills of Gusev Crater [39]; the MER Opportunity detected features that reveal ancient environmental conditions, and microscope observations indicate that ancient Meridiani once had abundant acidic groundwater and occasional liquid flow on the surface [40]; the Microscopic Imager on the Opportunity rover analyzed textures of soils and rocks at Meridiani Planum, and image mosaics of cross-stratification indicate that some sediments were deposited by flowing water [41]; Opportunity was commanded to explore Victoria Crater and found meteoritic debris near the crater rim [4]; Panoramic Camera images at Gusev Crater revealed a rock-strewn surface, and the spectra of some darker rock surfaces and rock regions exposed by brushing or grinding showed near-infrared spectral signatures consistent with the presence of mafic silicates such as pyroxene or olivine [42]. Scientists' selection of landing sites is also of great importance in determining the success of rover missions and the abundance of scientific findings [43].

(2) Scientists investigate the physical and mechanical properties of terrains that are essential for determining the wheel-terrain interaction mechanics of planetary rovers based on experimental results. Terrain property parameters such as particle size, density, internal cohesion, internal friction angle, and bearing strength could be used to estimate the traversability of rovers by simulation and optimization

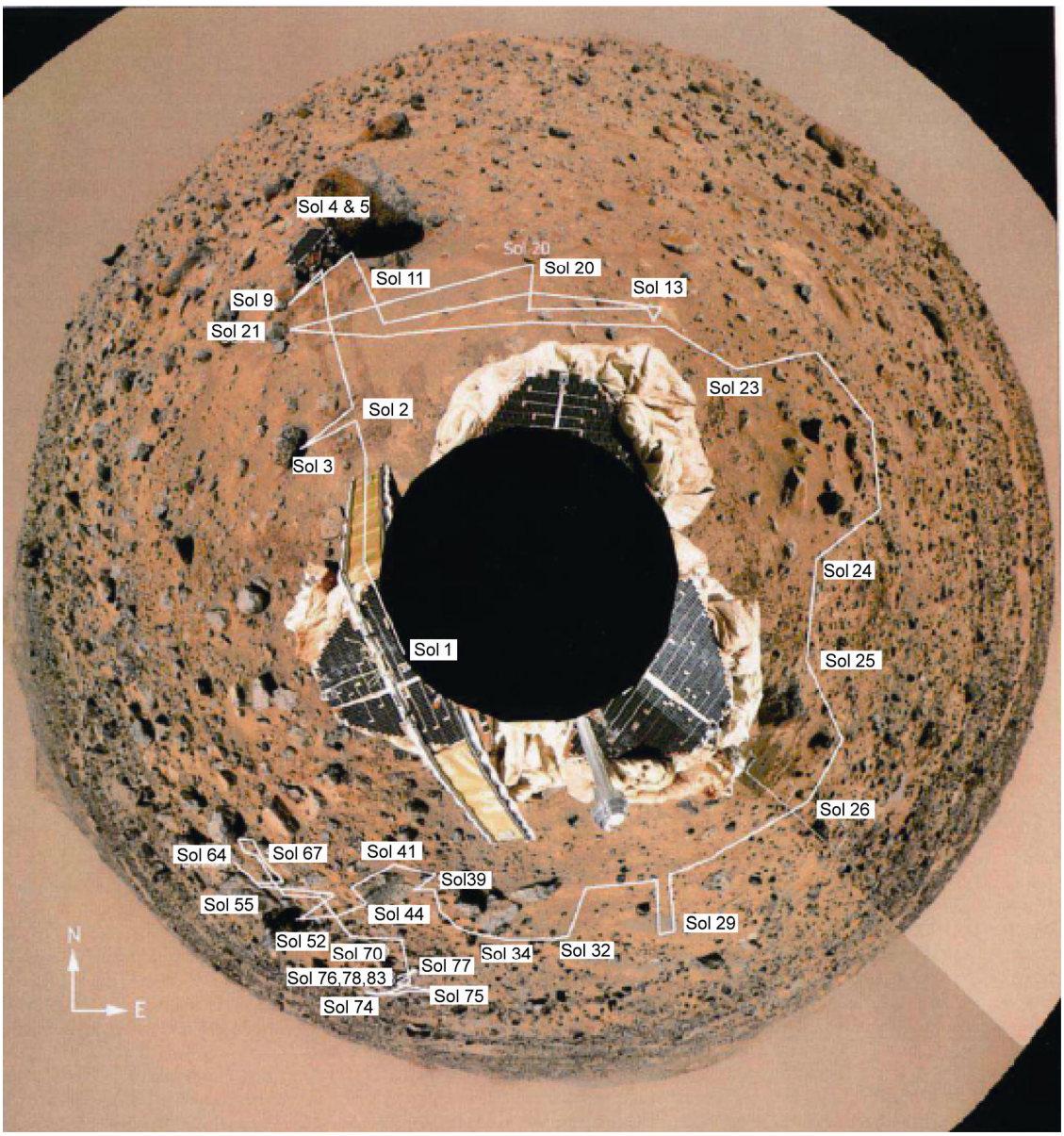

Figure 5 (Color online) Scientific missions planned for the Sojourner rover (the line shows the traversing trajectory) [38].

of the control strategy. Based on the experimental data obtained by the Sojourner rover, the rover team members characterized the Martian surface deposits and found that the soil-like deposits were similar to moderately dense soils on the Earth such as clayed silt with embedded sands, granules, and pebbles; the average bulk density of the deposits were near 1520 kg/m^3; the internal cohesion estimated by data fitting using the results of interaction mechanics experiments with wheels and various terrains (cloddy, dune, mixed, and compressible) ranged from –0.18 to 0.53 kPa, and the corresponding internal friction angle ranged from 42.4° to 26.4° [44]. The MER Spirit and Opportunity rovers measured surface temperatures in-situ using Mini-TES, based on which Robin et al. analyzed the thermal inertias to derive particle sizes, and compared the results with those measured directly using the Microscopic Imager; it was found that the bedforms on the floor of Bonneville Crater were covered with fine sand with particle diameters of approximately 160 mm; the surface of Laguna Hollow at Gusev Crater was silt 45 mm in diameter, the finest-grained material observed by the rovers [45]. Based on the measured sinkage of Opportunity's wheel track and the Mössbauer contact plate, Arvidson et al. estimated that Eagle Crater floor soils had an average bearing strength of 80 kPa with 5 kPa of internal cohesive and an internal friction angle of 20°, and the bearing strength and internal cohesion of the soils on the crater walls adjacent to the outcrops were one-tenth of those of Eagle Crater floor soils, although they had the same internal friction angles [46]; the corresponding values estimated from the data obtained by the Spirit rover

in the region in front of the drift Arena are 200 kPa, 15 kPa, and 25°, respectively [47].

3.2 Intelligence of engineers for planetary rovers

Engineers tell the planetary rovers "how to act" to realize the scientific goals by decomposing the mission tasks into command sequences that the rovers can execute autonomously. If the rovers encounter dangerous situations such as a stuck wheel, the engineers will attempt to help them to overcome such problems. According to the experience of driving Opportunity and Spirit rovers [18,31,48], for a supervisory tele-operated planetary rover, operators' intelligence is integrated into the rovers through the following steps with the help of HMIs.

(1) Analyze the data downlinked from the rovers and generate data for visualization, mission planning, and command sequence validation. The downlinked data include the current and historical states of a rover and imagery of terrains. Information on the rover's state is used to analyze and review the current state, identify anomalous issues, review previously commanded activities, and verify that the rover is ready to accept and perform a new set of the commanded activities [18]. Imagery is used to visually examine the surrounding terrain, identify hazards and areas of interest, specify targeting information for additional observations, and essentially present the operator with the least-processed view of the current environment [35]. Digital elevation maps (DEMs) of terrains are generated from the imagery information for 3D visualization and simulation. Figure 6 shows a graphical version of the MER rover in RSVP-HyperDrive generated from the downlinked data [49].

(2) Generate command sequences that can be executed effectively and safely by the rovers according to the science missions determined by scientists. Engineering team members assist the scientists in generating the science plan, build a detailed activity plan, generate a skeleton of command sequences and an animation showing the predicted activities of the locomotion system, arms, and scientific instruments based on virtual simulation, in order to verify that the rover activities match the understanding of the scientists and engineers. Then detailed command sequences are generated by the engineers, and are checked, reviewed, and fine-tuned by the engineers and scientists.

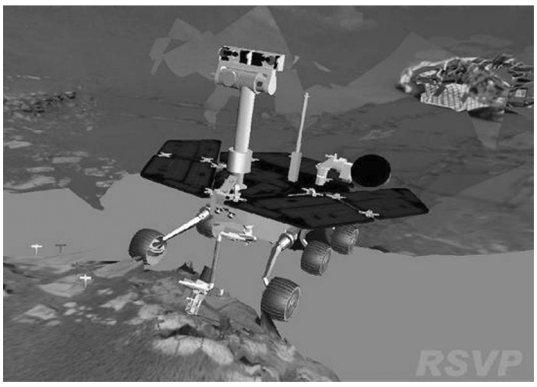

Figure 6 A graphical version of the MER rover displayed by RSVP-HyperDrive [49].

(3) Generate report products or remote team members to review by combining sequence commands and timing results from high-fidelity simulation, and uplink the command sequences to the planetary rovers.

(4) Supervise rover motion and send commands to the rovers to release them from difficulties, and update the autonomy of the rovers according to their experience during the rover operation. The Spirit rover is a good example [18]. On sol 343, the rover's right rear wheel dug into loose soil, and a rock was jammed between the inner surface of the wheel and the housing of the steering actuator. Engineers reconstructed the situation in the testbed at JPL, building slopes and digging trenches to test strategies for ejecting the rock and determining the maneuvering method to gradually extract the left rear wheel from the trench, eventually allowing the rock to fall out of the wheel as it rotated. According to this experience, engineers command the rovers to check their progress approximately every meter with VisOdom (visual odometry) to ensure that they encounter no excessive slip on challenging terrain. Combined drive techniques, including visual odometry, conditional overcommanding, slip checks, keepout zones, and "tricky drive," allowed Spirit to traverse slopes of up to 20° while tolerating slippage up to a preset limit of approximately 50%.

3.3 Double-layer HMIs

A double-layer HMI that could be used to integrate the intelligence of scientists and engineers into planetary rovers effectively and efficiently is shown in Figure 7. It was designed based on but not limited to the experience of the Mars rovers to make it suitable for supervisory tele-operated robots [17,18]. The Interactive Virtual Planetary Rover Environment, which is introduced in Section 5, could be used by scientists and engineers to realize direct tele-operation for robots such as lunar rovers with relatively small time delays.

One layer provides the interface for engineers and local scientists to accomplish supervisory tele-operation of autonomous planetary rovers, comprising rover analysis, visualization, and sequencing software. Downlinked data, including the images obtained by various cameras and the motion state information measured by sensors, are used to accomplish rover state analysis, image browsing, and terrain modeling (including geometric modeling of DEMs, and the terrain's physical and mechanical properties). Then the results can be used to support 3D visualization, immersion, and telepresence of the rover and terrain. Local scientists can use a science activity planner to design the science mission. A tactile activity planner can be used by engineers to generate initial command sequences and validate them by

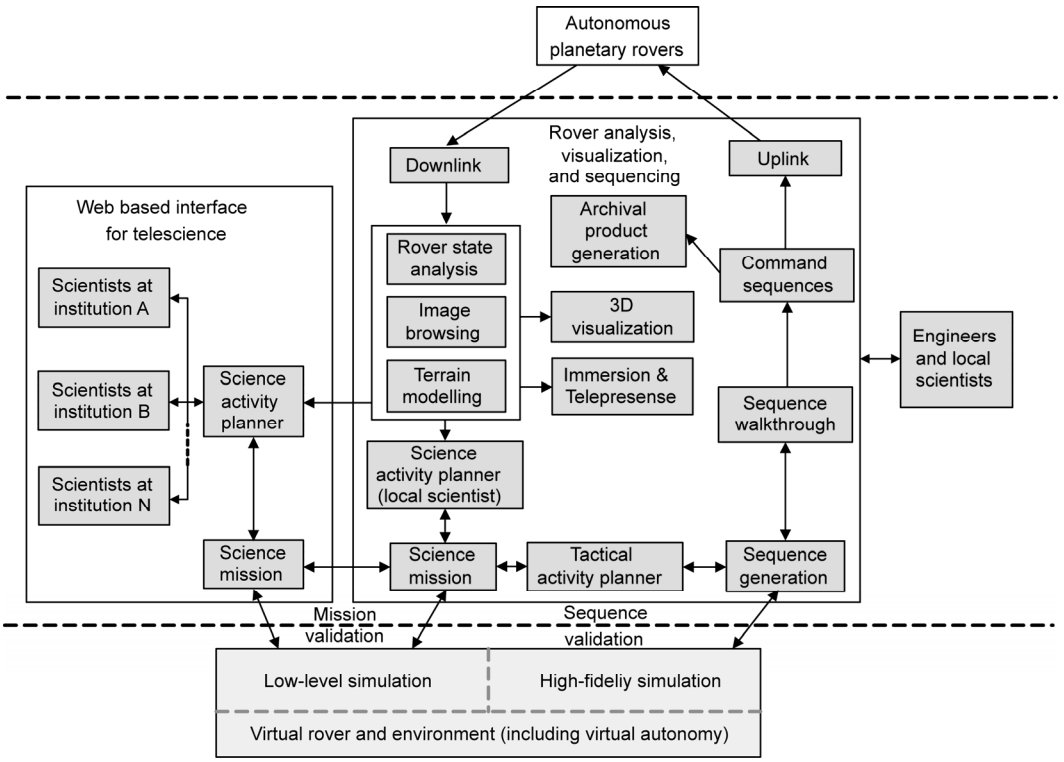

Figure 7 Architecture of double-layer HMIs for scientists and engineers (software).

high-fidelity simulation that involves the terramechanics, dynamics, and kinematics. The command skeleton will be broken down into details, and a walkthrough will then be done command-by-command by engineers and local scientists. Then the final command sequences will be generated together with an animation of the final validation, for creating archiving products, uplinking to rovers, and distributing to remote scientists.

The other layer of the double-layer HMI is a web-based interface for telescience that can be used by scientists at their homes or their institutions to work collaboratively with engineers and local scientists. During the long periods of rover missions, it is not practical for science team members to reside at the control center continually. They can make use of the downlinked results with an activity planner to construct scientific plans; the Science Activity Planner used by MER rovers is shown in Figure 8. Low-level (for instance, kinematics level) simulation can be used to perform faster-than-real-time predictions of their plans.

4 Robint: Intelligent perception, navigation, and motion control

This section summarizes the multilevel robotic intelligence architecture and key technologies of the functional layer: perception, navigation, and motion control. Most of the challenges that require high robint to arise from rough (geometry) and deformable (property) terrains. The physical and mechanical properties of deformable terrain have a significant influence on the locomotion of a rover. For example, while driving Spirit at Gusev Crater, Leger et al. found that the rover slipped 15%–20% on a 19° slope, but that it slipped 95% on a 16° slope 30m further; on some terrain, slip can also vary widely (from 10% to 60%) over successive 60 cm drive steps [31]. How to characterize the physical and mechanical properties of terrains with proprioceptive and exteroceptive information and apply the information to the motion control and navigation of planetary rovers is the most challenging and interesting problem yet to be solved.

4.1 Multilevel autonomy of planetary rovers

Typical robot and autonomy architectures composed of three levels—Functional, Executive, and Planner [50]—have been improved into the two-tiered CLARAty to support the autonomy of Mars rovers, as shown in Figure 9 [51]. The contents of the Decision Layer are introduced in refs. [51,52], and further details of CLARAty can be found in ref. [53]. The Decision Layer breaks down high-level goals into smaller objectives, arranges them in time based on known constraints and the system state, and accesses the appropriate capabilities of the Functional Layer to achieve the goals. The Functional Layer is an interface to the system hardware and its capabilities, including nested logical groupings and their resultant capabilities. These hardware capabilities are the interface through which the Decision Layer employs the

Figure 8 Science Activity Planner used by scientists to create desired activities for MER rovers [49].

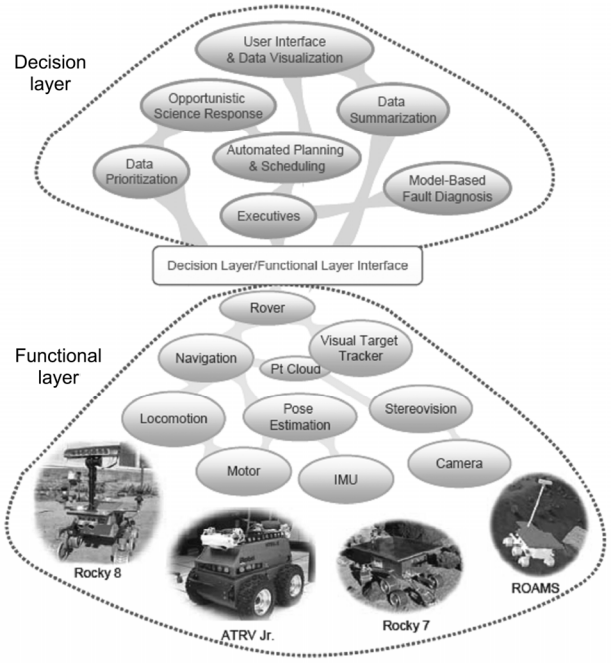

Figure 9 Coupled-Layer Architecture for Robotic Autonomy [51], including various types of generic technologies supported by each layer.

robotic system. This section focuses on the framework and technologies of the Functional Layer that are essential for the locomotion of planetary rovers. The double closed-loop architecture of locomotion autonomy for planetary rovers is shown in Figure 10.

4.2 Proprioception

One of the most challenging proprioception problems is to estimate the terrain properties and classify them based on the proprioceptive information for both scientific purposes and operational purposes [54,55]. Methods of estimating or identifying terrain parameters according to wheel-terrain interaction mechanics models have been developed by many researchers [56–59], but these approaches rely on the precision of the results such as slip ratio and contact forces that are fused from the proprioceptive information to a great extent [60–62]. The stereo odometry that will be introduced in the next subsection offers good precision in measuring the slip ratio of a rover [63], but the computation load is excessive, and it cannot estimate the slip ratios of different wheels. Theoretically, the linear velocity of each wheel can be predicted by fusion of kinematics information of the vehicle body and the passive joints, and the contact mechanics can be estimated by quasistatic analysis, but the precision levels are not yet ideal. Local terrain geometry and wheel sinkage are difficult to measure even with a visual method. If each wheel has a six-axis force/torque sensor installed at the wheel axle, the contact mechanics may be measured relatively easily. How to improve the proprioception precision and to apply the measured information to realize on-line terrain property characterization remain challenging issues. Figure 11 shows the architecture of three-loop terrain characterization in which the inner loop is realized in real-time to support control algorithm optimization by estimating the essential parameters (sinkage exponent and internal cohesion).

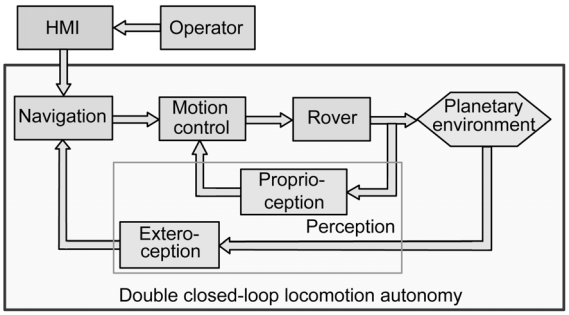

Figure 10 Double closed-loop architecture of locomotion autonomy of planetary rovers.

The middle loop is executed on-line when there is sufficient spectrum of slip ratios to identify other parameters (such as sinkage modulus, internal cohesion, deformation modulus, and contact angle coefficients) that are not sensitive to the contact mechanics. The outer loop is used to estimate and classify the terrain properties using image features and parameters and a learning algorithm, which will be introduced in the next subsection. A large amount of research must still be done before terrain characterization with three-loop algorithms can be realized.

4.3 Exteroception

The exteroception of both indoor and off-road mobile robots has been a hot research topic for many years. Localization (Where is the robot?) and terrain mapping (What is the terrain geometry?) are two basic problems. To solve the paradox of "to move precisely, a mobile robot must have an accurate environment map; however, to build an accurate map, the mobile robot's sensing locations must be known precisely" [64], SLAM (simultaneous localization and mapping) was put forward and has become a key approach to the navigation of off-road wheeled robots [65,66]. Visual information is widely used for the localization and mapping of mobile robots [67,68] and planetary rovers [69,70].

Compared with conventional vehicles, the difficulty of localization and mapping for planetary rovers lies in the high slip ratio, which arises from the coupling effects of terrain geometry and mechanical properties (deformability). Because the dead-reckoning method of estimating rover position is not accurate due to wheel slip, visual odometry has been used by planetary rovers successfully [71], but limited to special situations with off-line data processing because of the heavy computation load. Research efforts to find ways to realize real-time localization of rovers with high precision remain essential.

Planetary rovers have presented another challenge to the perception of WMRs that has attracted the interest of many researchers: the characterization of terrain with exteroceptive sensors for rover navigation. Simultaneous terrain characterization, terrain mapping, and localization is a potential topic of future research for off-road mobile robots that could improve robotic intelligence by adding a new dimension. Pioneering research has been carried out. Brooks and Iagnemma [72] proposed a self-supervised learning framework that enables a robotic system to predict the mechanical properties of terrains; a proprioceptive terrain classifier was designed to distinguish terrain classes based on features derived from rover-terrain interaction, and labels from the classifier were used to train a vision-based exteroceptive terrain classifier, which was in turn used to recognize similar terrain classes in stereo imagery [72]. However, Leger et al. reported that high-resolution PanCam (Panoramic Camera) imagery of regions where the Spirit rover experienced slips of 15%–20% on a 19° slope and slips of 95% on a 16° slope showed no difference in terrain appearance [31]. New approaches should be developed to compensate for the drawbacks of stereo vision methods; for example, surface temperatures measured by Mini-TES could be applied to estimate particle diameters to support terrain classification [45], and experiments using terrestrial WMRs have verified that infrared and ultrasonic range sensors could be used to classify terrains [73].

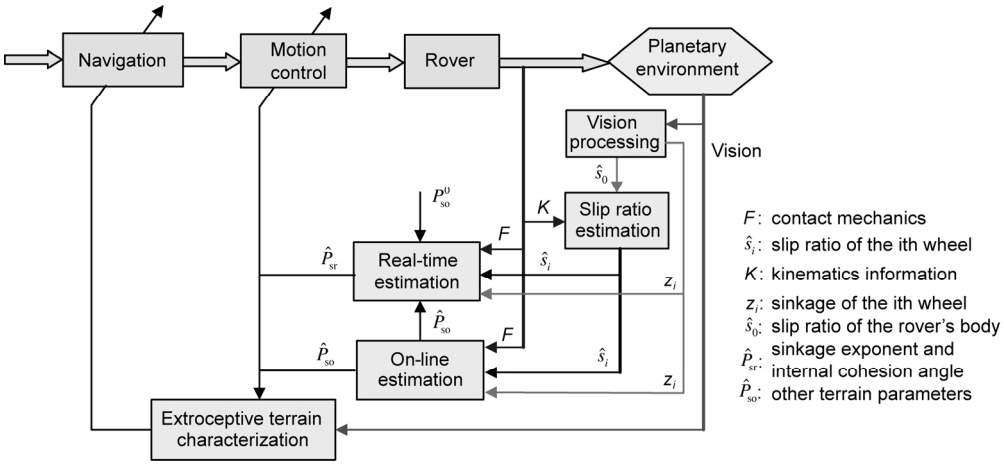

Figure 11 Three-loop terrain characterization.

4.4 Navigation

The navigation of planetary rovers [74] mainly involves terrain traversability analysis and path planning. Lacroix et al. proposed a rover navigation approach on unknown rough terrains [75], and Maimone et al. proposed a method of terrain assessment (Figure 12) and path selection for autonomous navigation of MER rovers [13]. Compared with terrain geometry, the mechanical properties of terrain have a greater influence on the trafficability of rovers [76] and must be considered in rover navigation.

How to predict the traversability of a rover while following and evaluating potential paths for selecting the optimal one with consideration of wheel-terrain interaction mechanics is a key challenge. Iagnemma et al. proposed a rapid physics-based path planning approach that takes into account uncertainty in the robot model, terrain model, and range sensor data [77]. Ishigami et al. [78] presented a path evaluation method that considers the wheel slip dynamics of planetary exploration rovers by comparing the values of criteria functions calculated using the path-following results in dynamic simulation. Howard and Kelly developed an algorithm with high generality and efficiency for trajectory generation of WMRs with application to planetary rovers that could accommodate the effects of rough terrain, vehicle dynamics, and wheel–terrain interaction [79], as shown in Figure 13.

With the progress of the related key technologies such as terrain characterization methods and wheel–terrain interaction mechanics models, new autonomous navigation approaches will be developed to ensure that rovers are able to traverse rough and deformable terrains more efficiently and safely, and artificial intelligence such as fuzzy logic [80], [81] and neural networks [82] will be integrated into the navigation system of planetary rovers.

4.5 Motion control

Intensive research has been carried out for many years aiming at control problems encountered by WMRs, because they are considered to be typical nonholonomic systems [83,84]. Despite fruitful theoretical results on stabilization, path following, and trajectory tracking for conventional terrestrial WMRs with assumptions of flat hard terrain without slipping and skidding, planetary rovers present many new challenges such as redundant control (six driving motors with four steering motors to drive with three degrees-of-freedom mobility), rough terrain control, slipping, and skidding due to deformable characteristics of terrain.

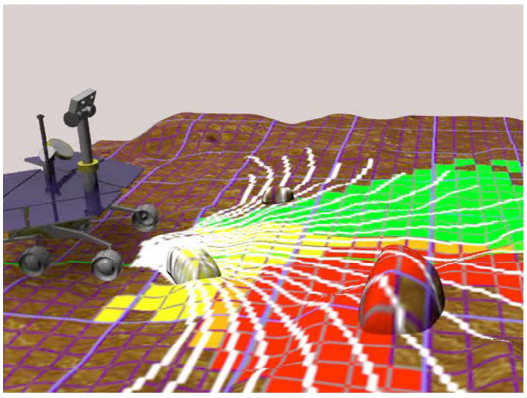

Figure 12 (Color online) Traversability map: grid cell goodness evaluations and possible paths [13]; the tall rocks are assigned "impassable" evaluations in red, medium rocks are assigned "moderate" evaluations in yellow, and flat areas are assigned "perfect" evaluations in green.

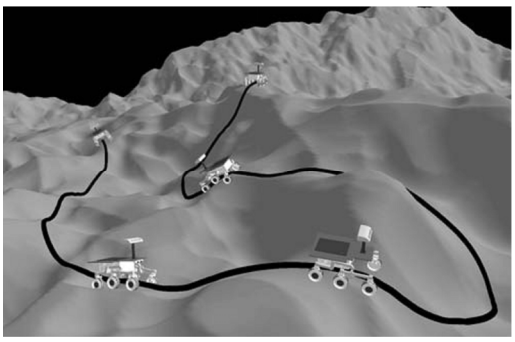

Figure 13 Trajectory planning on the rough terrain of Mars [79].

Although six-wheeled rocker-bogie rovers have been controlled successfully for traversing Mars, theoretical research has been insufficient, and methods for improving driving efficiency and decreasing wheel dynamic sinkage are lacking. Physics-based control algorithms must be developed by considering not only the kinematics and dynamics but also the terramechanics to enhance mobility on rough and deformable terrain [85]. Advanced rover control algorithms are expected to be developed to realize robust and optimal control and to follow a planned path with high energy efficiency. Human intelligence in driving rovers to avoid wheel stuck and to escape from dangerous situations, as reported by the operators of Mars rovers, could also be integrated into the algorithms. Figure 14 shows the advanced rover control architecture that should be realized in order to enhance the mobility of future planetary rovers that traverse challenging off-road terrains.

The rovers should have the ability of following a planned path autonomously in order to avoid obstacles and arrive at the destination successfully. To follow the path and decrease the deviation distance caused by lateral skidding of wheels, the steering motors should be controlled coordinately [86,87]. Wheel slip should also be measured and compensated [88–90] to maintain the velocity of the rovers and, more importantly, to coordinate the angular velocities of wheels' driving motors and decrease the "fight" among wheels, thus improving energy efficiency [91] and avoiding wheel stuck caused by slip-sinkage. A path-following algorithm and slip-compensation algorithm could be combined to generate the angular velocities of both the steering motors and the driving motors [92].

The current physics-based control algorithms for planetary

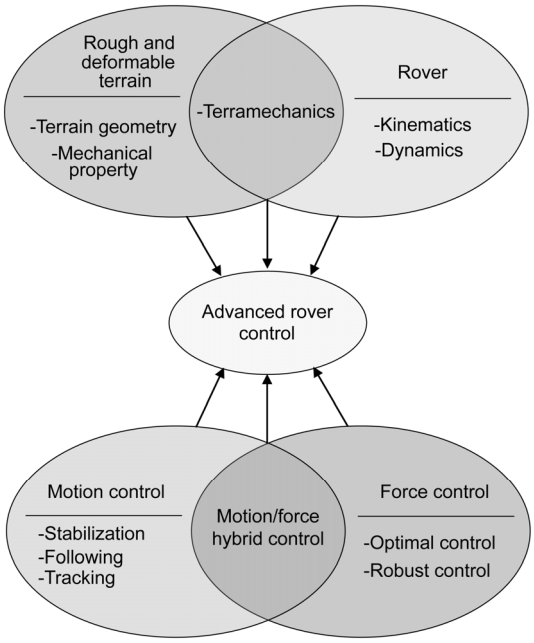

Figure 14 Architecture of advanced control for planetary rovers on deformable and rough terrain.

rovers traversing rough and deformable terrains are ad hoc solutions, lacking complete theoretical analysis. Fruitful results for conventional nonholonomic WMRs could be used to support the development of control algorithms from the perspective of control theory. Initial research has been carried out to fill the gap between the engineering requirements and control theory, including the backstepping control of nonholonomic wheeled robots on slopes [93], and analysis of slipping and skidding of the wheeled robots on the kinematics level [94] and terramechanics level [95] from the control design perspective. However, such efforts are still at an early stage of realizing optimal and robust force/motion hybrid control of nonholonomic planetary rovers based on kinematics, dynamics, and terramechanics as indicated in Figure 14.

5 Virtint: Intelligent virtual rover interacting with virtual planetary terrain

Several examples of simulation software that could predict the mobility of intelligent virtual planetary rovers traversing virtual planetary terrain have been developed to support the tele-operation of planetary rovers [96]. ROAMS was developed by Yen et al. [97] for the MER rovers, and the CLARAty software could be used to realize the autonomy of virtual rovers [98]. Recently, Zhou et al. [99] developed a software tool entitled Artemis (Adams-based Rover Terramechanics and Mobility Interaction Simulator) that can simulate the motion of rovers with high slippage and sinkage, in order to help evaluate mobility of Mars rovers on candidate paths. RSVP contains two main components—ROSE (Rover Sequence Editor) and Hyperdrive—and the latter is an immersive 3D simulation of the rover that enables operators to construct detailed rover motions and verify their safety [18]. Schäfer et al. [100] simulated planetary rover mobility on soft and uneven terrain and carried out experimental validation on the basis of the future European Mars rover mission ExoMars.

A double-level simulation architecture that supports faster-than-real-time simulation and high-fidelity simulation is proposed in this section, and three key aspects of its realization—virtual rover, virtual terrain, and wheel-terrain interaction mechanics—are summarized.

5.1 Double-level virtual simulation

Figure 15 shows the operation of the double-level simulation software RoSTDyn [96], which was developed for the analysis of China's Yutu lunar rover. The low-level simulation is based on kinematics and can be used by scientists through the science activity planner to detect the geometrical impact with a faster-than-real-time speed while executing the planned activities. The high-fidelity simulation is based on terramechanics, dynamics, and kinematics to support the 3D predictive display for direct tele-operation of lunar rovers. If the scientific "goals" are sent to the rovers directly, the virtual rover will move in Autonomous Navigation (AutoNav) mode based on virtual stereo vision; if "paths" such as line, arc, and steering-in-place are sent to the rover, the Locomotion mode will be executed, and the Motor Control mode will drive the motors directly by setting their "positions." Figure 16 shows the simulation snapshots of China's Yutu lunar rover in RoSTDyn.

Engineers can use the Interactive Virtual Planetary Rover Environment program to realize direct tele-operation of lunar rovers by comparing the feedback motion of an actual lunar rover with that of the virtual lunar rover predicted by RoSTDyn. The virtual motion is ahead of the actual motion in terms of a twofold time delay, which could be increased further by setting an additional time delay before the command sequences are sent, and decreased by setting a time delay to the virtual rover. The mechanical and physical properties of the terrain are expected to be estimated using the proprioception information and imagery from the rover based on terramechanics.

5.2 Virtual planetary terrain modeling

Characterizing the terrain with which the rover intimately interacts is important in simulation. Planetary terrain contains two types of information that influence the locomotion of rovers: one type comprises physical and mechanical properties as described earlier, and the other is terrain geometry, as described in this subsection.

The DEM of terrain meshes is usually used to describe the geometry of terrain [35,98,101]. Raw camera images

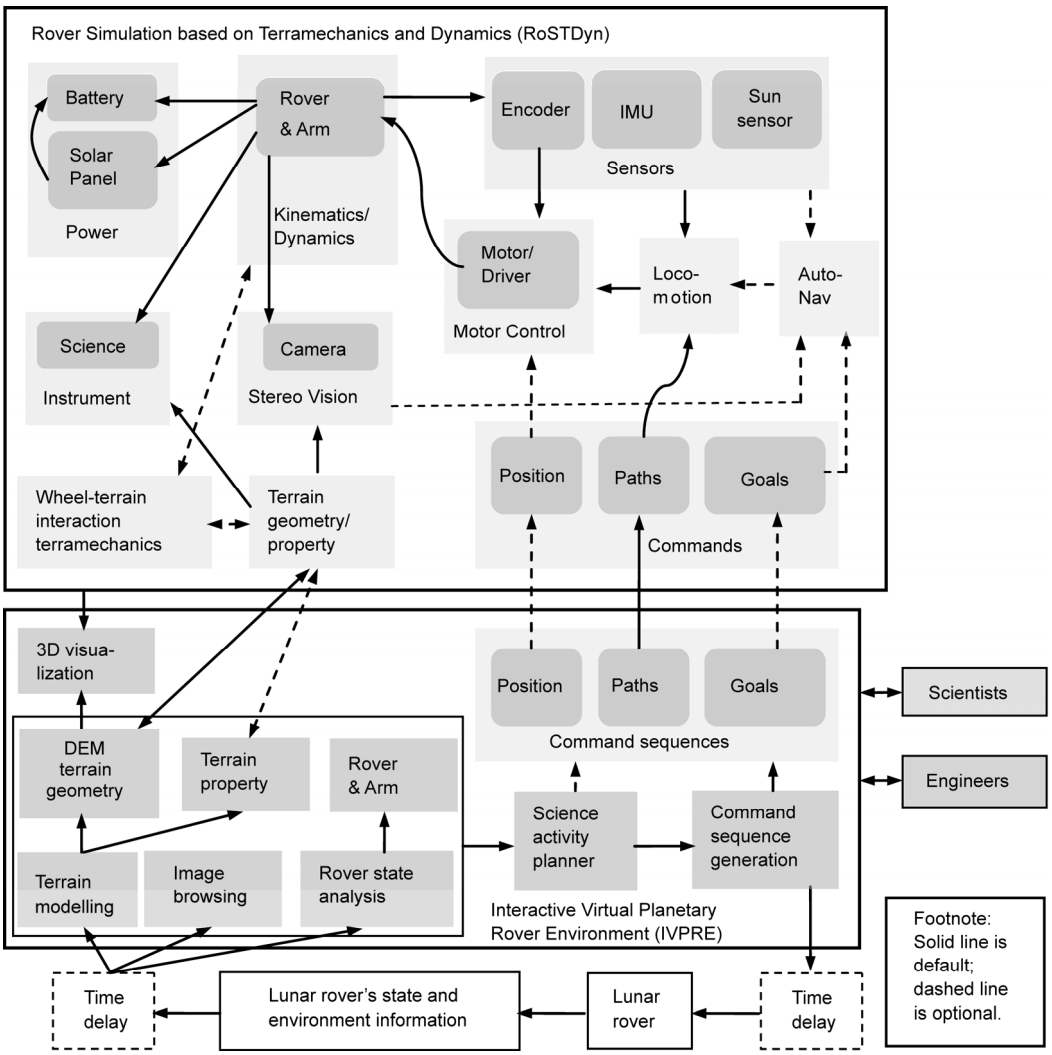

Figure 15 Rover Simulation based on Terramechanics and Dynamics (RoSTDyn) and its application to direct tele-operation of lunar rovers with the aid of Interactive Virtual Planetary Rover Environment.

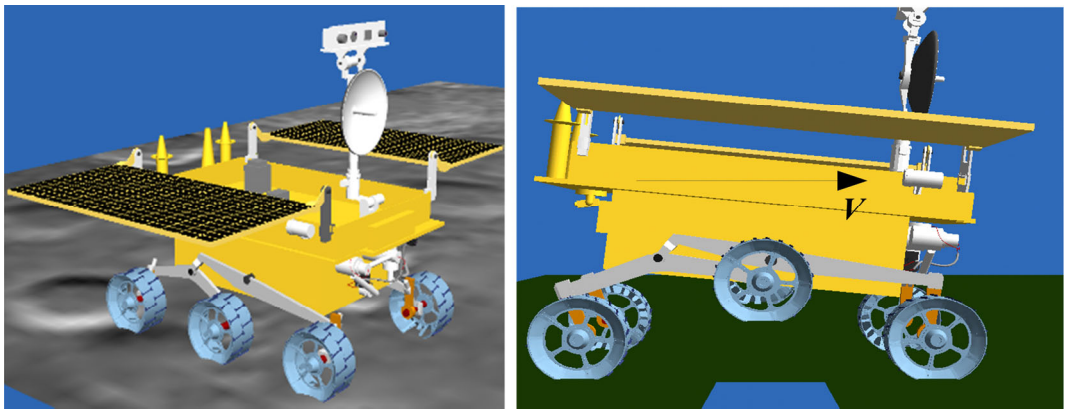

Figure 16 (Color online) Snapshots of rover simulation in RoSTDyn [96].

can aid rover operators' understanding of environments through visualization, but such images cannot be used directly in simulation. Terrain meshes must be generated from imagery of stereo cameras on the rovers, such as panoramic cameras, navigation cameras, and hazard avoidance cameras. Left and right imagers generate stereo pairs for producing 3D terrain models, and Wright et al. [102] described the processing performed on the stereo pairs. Each stereo pair is

first processed with a correlator that produces a disparity map that identifies matching features in each image. The camera model is then used to compute the range to each pixel in one image using the disparity to its matching pixel in the other image. Then, the camera pointing information is used to project the pixels to an (*x*, *y*, *z*) location in 3D space. Several image-derived products specialized for rover simulation, visualization, and operations are presented in detail in refs. [103,104]. LiDAR (Light Detection And Ranging) could also be used to model the terrain DEM [105] with the advantage of superior resolution and range, but LiDAR lacks imagery information for immersion and telepresence and requires relatively more energy. The LiDAR-based systems have been successfully used in space missions and thus are space qualified. Patrick et al. [106] developed a long-range rover localization approach by matching LiDAR scans to orbital elevation maps. The physical and mechanical properties of terrains can also be characterized on the Earth based on the on-board approaches for rovers. Because the computation ability for virtual intelligence is much higher than that for rover autonomy, more complicated and intelligent methods could be developed further.

5.3 Virtual intelligent rover

A virtual intelligent rover should behave as a real rover with high fidelity, the technologies of which are illustrated in Figure 15. Virtual rovers should simulate the properties of real rovers, including kinematics, dynamics, terramechanics, power, motor, scientific instruments, and sensors. On the other hand, virtual rovers should have virtual robotic intelligence, developed according to robotic intelligence but improved to adapt to the virtual environment. Kinematics, dynamics, and terramechanics are all essential for the high-fidelity simulation of a rover. General kinematics and dynamics modeling of planetary rovers is described in this subsection, and the terramechanics will be summarized in the next subsection.

Planetary rovers are articulated multibody systems with a moving base and n_w end-points (wheels). Let $\boldsymbol{q}=[q_1\ q_2\cdots\ q_{n_v}]^T$ denote the joint variables, where n_v is the number of joints. Let $\boldsymbol{q}_s=[q_l\ q_m\ q_n\ \mathrm{L}\ q_s]^T$ denote a branch from the rover body to a wheel, and n_s denote the number of elements in $\boldsymbol{q}_s$. Replace the joint number l, m, n, ⋯, s of the branch with 1, 2, 3 ⋯, n_s, as shown in Figure 17, which also shows the inertial coordinates $\{\Sigma_I\}$, and coordinates $\{\Sigma_i\}$ attached to link i (i=l, m, n, ⋯, s) and related vectors, where $\boldsymbol{p}_i$ is the position vector of link i, $\boldsymbol{r}_i$ is the position vector of the centroid of link i, $\boldsymbol{c}_{ij}$ is the link vector from link i to joint j, $\boldsymbol{l}_{ij}=\boldsymbol{p}_j-\boldsymbol{p}_i$ is the link vector from joint i to joint j, and $\boldsymbol{l}_{ie}$ is the vector from joint i to end-point e.

The kinematic equations can be deduced with the recursive method for each branch [101,107], to calculate the velocities of each body's center of mass and those of the centers of wheels. The velocities of all the branches can then be combined to formulate the general kinematic equation of a rover.

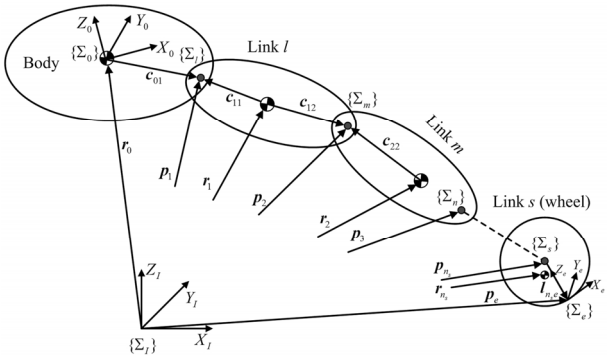

Figure 17 Coordinates and vectors from rover body to a wheel [101]

Let $\dot{\boldsymbol{\Phi}}=\left[\begin{pmatrix}\boldsymbol{v}_0^T & \boldsymbol{\omega}_0^T\end{pmatrix}\ \dot{\boldsymbol{q}}^T\right]^T$, which is a vector with (6+nv) elements, consisting of the linear velocity and angular velocity of the body, and the joint velocity. If we let $\dot{\boldsymbol{X}}_{ae}$ and $\boldsymbol{J}_{ae}$ denote the velocities of all the wheel centers and the corresponding Jacobian matrix, which are a $6n_w\times1$ vector and a $6n_w\times(n_v+6)$ matrix, respectively, we obtain

$$\dot{\boldsymbol{X}}_{ae}=\boldsymbol{J}_{ae}\dot{\boldsymbol{\Phi}}. \tag{1}$$

The same method is used to deduce the Jacobian matrix of mapping the velocity from the generalized coordinates to the link centroid, and the following equation is obtained:

$$\dot{\boldsymbol{X}}_a=\boldsymbol{J}_a\dot{\boldsymbol{\Phi}}, \tag{2}$$

where $\dot{\boldsymbol{X}}_a$ ($6n_v\times1$) is the velocity vector of all of the centroids, and $\boldsymbol{J}_a$ ($6n_v\times(n_v+6)$) is the Jacobian matrix.

According to the Lagrange function,

$$\boldsymbol{N}+\boldsymbol{J}_{\mathrm{ae}}^T\boldsymbol{N}_{\mathrm{ae}}=\boldsymbol{H}_{\mathrm{sys}}(\boldsymbol{\Phi})\ddot{\boldsymbol{\Phi}}_{\mathrm{sys}}+\boldsymbol{C}(\boldsymbol{\Phi},\dot{\boldsymbol{\Phi}})\dot{\boldsymbol{\Phi}}+\boldsymbol{f}(\dot{\boldsymbol{\Phi}})+\boldsymbol{G}(\boldsymbol{\Phi}), \tag{3}$$

where $\boldsymbol{C}$ is a $(n_v+6)\times(n_v+6)$ stiffness matrix describing the Coriolis and centripetal effects, which are proportional to $\dot{q}_i^2$ and $\dot{q}_i\dot{q}_j$, respectively; $\boldsymbol{f}$ is a $(n_v+6)\times1$ matrix that describes viscous and coulomb friction, negligible for rigid-body dynamics system; $\boldsymbol{G}$ is a $(n_v+6)\times1$ gyroscopic vector reflecting the gravity loading; and $\boldsymbol{F}_{\mathrm{sys}}$ is the vector of generalized forces:

$$\boldsymbol{F}_{\mathrm{sys}}=\boldsymbol{N}+\boldsymbol{J}_{ae}^T\boldsymbol{N}_{ae}, \tag{4}$$

where $\boldsymbol{N}$ is a $(n_v+6)\times1$ matrix including the forces ($\boldsymbol{F}_0$)/moments ($\boldsymbol{M}_0$) acting on the body and those acting on the joints ($\boldsymbol{\tau}=[\tau_1\ \ \tau_2\ \ \cdots\ \ \tau_{n_v}]^T$, and $\boldsymbol{N}_{ae}$ is a $6n_w\times1$ vector including the external forces ($\boldsymbol{F}_e$) and moments ($\boldsymbol{M}_e$) of the soil acting on the wheel.

If we let $\boldsymbol{C}(\boldsymbol{\Phi},\dot{\boldsymbol{\Phi}})\dot{\boldsymbol{\Phi}}+\boldsymbol{f}(\dot{\boldsymbol{\Phi}})+\boldsymbol{G}(\boldsymbol{\Phi})=\boldsymbol{E}$, the generalized

accelerations can be calculated according to eq. (3) as

$$\ddot{\boldsymbol{\Phi}}_{\text{sys}} = \boldsymbol{H}_{\text{sys}}^{-1}(\boldsymbol{N} + \boldsymbol{J}_{ae}{}^{\text{T}}\boldsymbol{N}_{ae} - \boldsymbol{E}) . \quad (5)$$

The recursive Newton-Euler method is used to deduce an equivalent dynamics equation to eq. (3) [96,107].

If we let $\ddot{\boldsymbol{\Phi}}_{\text{sys}} = 0$ and $\boldsymbol{N}_{ae} = 0$, $\boldsymbol{E}$ can be calculated recursively in simulation. We can substitute E into eq. (5) to calculate the acceleration, which is then integrated to predict the velocity and position of the joints step by step.

If the contact is between the scientific instruments and the terrain, such as in the case of the Rock Abrasion Tool, the contact force should also be considered. Kinematics of robotic arms, such as with the Instrument Deployment Device, can also be deduced with a similar method.

5.4 Wheel-terrain interaction mechanics of rovers

The modeling of wheel-terrain interaction comprises two parts: geometrical contact and interaction mechanics, corresponding to the terrain geometry and mechanical properties, respectively.

(1) Geometrical Contact Calculation. Calculating the interaction area of a wheel moving on soft soil is important for high-fidelity simulation, based on which the interaction mechanics can be predicted and transformed. Figure 18(a) shows the interaction area of a wheel moving on rough terrain. The known parameters are: (x_w, y_w, z_w), which is the position of a wheel's center w; φ_w, which is the yaw angle of a wheel; and the DEM of the terrain. The interaction area is simplified as an inclined plane determined by points P_1, P_2, and P_3. The equation of the inclined plane $P_1P_2P_3$ is

$$A_t(x - x_1) + B_t(y - y_1) + C_t(z - z_1) = 0 . \quad (6)$$

Equations of predicting the coordinates of points P_1, P_2, P_3 and A_t, B_t, C_t are presented in ref. [101]. The contact can be considered as a wheel with a simplified slope determined by points P_1, P_2, P_3, as shown in Figure 18 (b), where $\{\Sigma_e\}$ and $\{\Sigma_w\}$ are coordinate systems with the same orientation and different origins, at the end point and wheel center, respectively. The wheel sinkage is then determined by

$$z = r - \frac{\left|A_t(x_w - x_1) + B_t(y_w - y_1) + C_t(z_w - z_1)\right|}{\sqrt{A_t^2 + B_t^2 + C_t^2}} . \quad (7)$$

The contact can be decomposed into climbing up a slope with angle θ_{cl} and crossing a slope with angle θ_{cr}:

$$\begin{cases} \theta_{cl} = \arcsin[(-A_t - B_t \tan\varphi_w)/X_1] \\ \theta_{cr} = \arcsin[C_t(A_t \tan\varphi_w - B_t)/X_2] \end{cases}, \quad (8)$$

where $X_1 = \sqrt{C_t^2(1 + \tan^2\varphi_w) + (A_t + B_t \tan\varphi_w)^2}$ and $X_2 = \sqrt{X_3[A_t^2 + C_t^2 + 2A_tB_t \tan\varphi_w + (B_t^2 + C_t^2)\tan^2\varphi_w]}$.

The transformation matrix from $\{\Sigma_e\}$ to $\{\Sigma_I\}$ is

$$\boldsymbol{A}_e = \begin{bmatrix} \frac{C_t}{X_1} & \frac{-A_tB_t - (B_t^2 + C_t^2)\tan\varphi_w}{X_2} & \frac{A_t}{X_3} \\ \frac{C_t \tan\varphi_w}{X_1} & \frac{C_t^2 + A_t^2 + A_tB_t \tan\varphi_w}{X_2} & \frac{B_t}{X_3} \\ \frac{-A_t - B_t \tan\varphi_w}{X_1} & \frac{A_tC_t \tan\varphi_w - B_tC_t}{X_2} & \frac{C_t}{X_3} \end{bmatrix}, \quad (9)$$

where $X_3 = \sqrt{A_t^2 + B_t^2 + C_t^2}$. Let ${}^e\boldsymbol{F}_e$ and ${}^e\boldsymbol{M}_e$ denote the wheel-terrain interaction forces and moments, respectively, that act on the wheel in the coordinate $\{\Sigma_e\}$. The equivalent forces and moments that act on the wheel in the inertial coordinate $\{\Sigma_I\}$ are

$$\begin{cases} \boldsymbol{F}_e = \boldsymbol{A}_e{}^e\boldsymbol{F}_e , \\ \boldsymbol{M}_e = \boldsymbol{A}_e{}^e\boldsymbol{M}_e . \end{cases} \quad (10)$$

(2) Wheel-Terrain Interaction Mechanics. The soil applies three forces and three moments to each wheel, as shown in Figure 19. The normal force, denoted by F_N, can sustain the wheel. The cohesion and shearing of the terrain

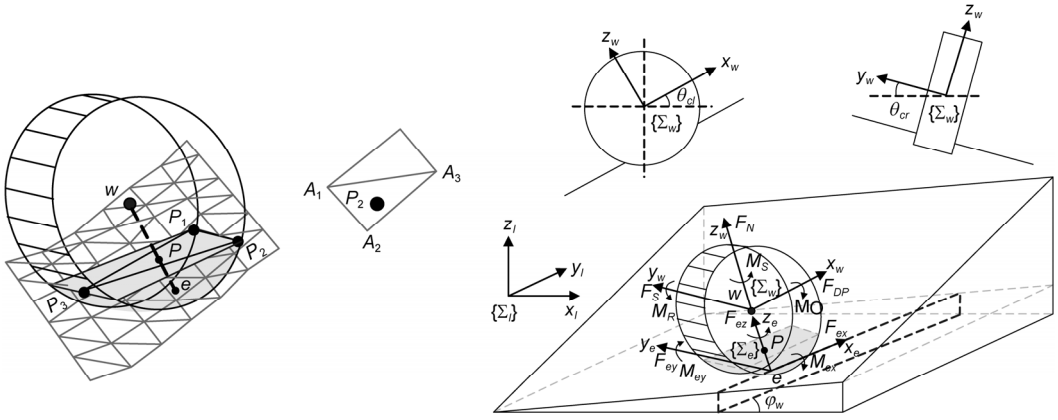

(a) Interaction of wheel and deformable terrain (b) Force of a wheel moving on a simplified slope

Figure 18 Interaction geometry and mechanics of a wheel on deformable terrain [96,101].

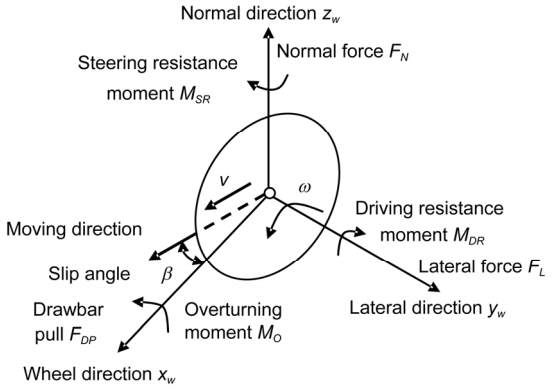

Figure 19 Wheel-soil contact mechanics [108].

can generate a resistance moment M_{DR} and a tractive force. A resistance force is produced because the wheel sinks into the soil. The combined net force of the tractive and resistance forces is called the drawbar pull F_{DP}, which is the effective force of a driving wheel. When a wheel steers or the terrain is rough, the skid angle β is generated to produce a lateral force F_L, steering resistance moment M_{SR}, and overturning moment M_O on the wheel.

The wheel-soil contact mechanics are influenced by the soil properties, wheel properties, terrain geometry, and motion state variables. Therefore a generalized form for wheel-soil contact mechanics is

$$\begin{cases} F_N = F_{zw} = F_N(P_S, P_T, P_W, P_M) = W, \\ F_{DP} = F_{xw} = F_{DP}(P_S, P_T, P_W, P_M) = f_{DP}, \\ F_L = F_{yw} = F_{\mathrm{L}}(P_S, P_T, P_W, P_M), \\ M_{\mathrm{O}} = M_{xw} = M_{\mathrm{O}}(P_S, P_T, P_W, P_M), \\ M_{DR} = -M_{yw} = M_{DR}(P_S, P_T, P_W, P_M) = T_D, \\ M_{SR} = -M_{zw} = M_{SR}(P_S, P_T, P_W, P_M) = T_S, \end{cases} \tag{11}$$

where W is the vertical load, f_{DP} is the resistance force, T_D is the driving torque generated by the driving motor and gears, and T_S is the steering torque generated by the steering mechanism.

The soil interacts with a wheel in the form of continuous normal and shearing stresses. The functions in eq. (11) are relatively complex because they are the integration of stresses, which are influenced by numerous parameters. To deduce the detailed form of eq. (11) to predict the wheel-soil contact mechanics with high fidelity, the equations of normal stress and shearing stress should be obtained first based on theoretical analysis and experimental study. When a model with considerable fidelity is obtained, the unknown parameters can be estimated with inverse functions of eq. (11) if the wheel-soil interaction forces and moments are measured or given, and can in turn be used for high-fidelity rover simulation.

The terramechanics developed for conventional terrestrial vehicles [109,110] provide the foundation of wheel-terrain interaction mechanics for planetary rovers and are usually directly used; however, there are many differences between rovers and conventional vehicles in terms of the wheel dimensions, motion state, payload, running environment, velocity, chassis configuration, etc., which result in large differences in their terramechanics [111]. For example, WMRs violate almost all the conditions that Bekker [109] pointed out for the application of his model; conventional pressure–sinkage relationship equations are based on static state experiments and are incapable of reflecting the dynamic process during the interaction of a wheel and terrain. An overview of the terramechanics for planetary exploration WMRs can be found in ref. [111]. Some typical and recent research results will be discussed here.

Experiments were carried out to investigate slip-sinkage, lug effect, dimension effect, and load effect during the interaction of planetary rovers' wheels and a planetary soil simulant [112], and improved models that could reflect multiple effects were deduced and validated by experiment [113,114]. Meirion-Griffith and Spenko proposed a modified pressure–sinkage model for small and rigid wheels on deformable terrains [115]. Irani et al. developed a dynamic terramechanic model for small and lightweight vehicles in sandy soils considering the fluctuation of contact mechanics due to the wheel lugs [116]. Preliminary study of longitudinal skid mechanics for wheels of planetary rovers was performed, including experiments, modeling, and comparison with slip mechanics [117,118]. Ishigami et al. deduced a model to predict the lateral force of rovers' wheels with lateral skid [86]; Ding et al. comprehensively investigated steering sinkage and steering resistance moment by considering the multiple effects on the wheels of planetary rovers [108].

The equations in integral form of the normal and shear stresses are complex. To improve calculation speed, closed-form analytical equations have been derived [58,119,120], which could also be used for improving robotic intelligence. Despite recent research conducted on rover terramechanics, much remains to be done if a systematic theory is to be formulated.

6 Summary and conclusions

(1) There is a long way to go before rovers may evolve into robotic scientists and engineers capable of exploring planets with little intervention from humans. The three-layer robint-humint-virtint intelligence architecture, which integrates human intelligence into robotic intelligence with the help of virtual intelligence, is already standard and applicable to planetary exploration rovers such as the Mars and lunar rovers.

(2) The intelligence of scientists in mission planning and that of engineers in generating command sequences to drive rovers safely and efficiently may be integrated into planetary rovers by means of double-layer HMIs, i.e., with the

web-based interface for telescience and with the rover analysis, visualization, and sequencing program.

(3) Robotic intelligence features a multi-level autonomy architecture. The functional layer has key technologies of perception (proprioception and exteroception), navigation (path planning and evaluation), and motion control. The physical and mechanical properties of rough and deformable terrains present the most challenging issues to improving robint; for example, SLAM for WMRs must evolve to enable not only simultaneous localization and mapping but also terrain characterization.

(4) Virtint is composed of the double-level virtual simulation of planetary rovers, i.e., faster-than-real-time kinematics simulation and high-fidelity simulation based on terramechanics, dynamics, and kinematics, to support command generation and validation for scientists and engineers. The virtual planetary environment, virtual intelligent rover, and wheel-terrain interaction are the three basic components. The wheel-terrain interaction includes contact geometry and interaction mechanics, which are key in determining the mobility of rovers, but as yet lack a systematic theory.

(5) The architecture of the three-layer intelligence based on planetary exploration rovers may be generalized for use by other space systems (such as on-orbit manipulator [121]) and robotic systems (such as the legged robots [122]) that require tele-operated commands with a certain time delay.

This work was supported by the National Natural Science Foundation of China (Grant No. 61370033), National Basic Research Program of China (Grant No. 2013CB035502), Foundation of Chinese State Key Laboratory of Robotics and Systems (Grant Nos. SKLRS201401A01, SKLRS-2014-MS-06), the Fundamental Research Funds for the Central Universities (Grant No. HIT.BRETIII.201411), Harbin Talent Programme for Distinguished Young Scholars (No. 2014RFYXJ001), Postdoctoral Youth Talent Foundation of Heilongjiang Province, China (Grant No. LBH-TZ0403) and the "111 Project" (Grant No. B07018).

1 Robinson M. Soviet Union lunar rovers. http://lroc.sese.asu.edu/posts/11
2 JPL. NASA/JPL Mars pathfinder. http://marsprogram.jpl.nasa.Gov/MPF/
3 JPL. NASA/JPL Mars exploration rover mission. http:// marsrovers.jpl.nasa.gov/home/index.html
4 Squyres S W, Knoll A H, Arvidson R E, et al. Exploration of victoria crater by the Mars rover opportunity. Science, 2009, 324: 1058–1061
5 Squyres S W, Arvidson R E, Bell III J F, et al. The Spirit rover's Athena science investigation at Gusev Crater, Mars. Science, 2004, 305: 794–799
6 JPL. Mars Science Laboratory–Curiosity: NASA's next Mars rover. http://www.nasa.gov/mission_ pages/msl/
7 ESA. ExoMars Mission. http://www.esa.int/ SPECIALS/ExoMars/SEM10VLPQ5F_0.html
8 Sun Z Z, Jia Y, Zhang H. Technological advancements and promotion roles of Chang'e-3 lunar probe mission. Sci China Tech Sci, 2013, 56: 2702–2708
9 JAXA. Moon lander SELENE 2. http://www. jspec.jaxa. jp/e/activity/selene2.html
10 NASA. Solar System exploration–the 2006 Solar System exploration roadmap for NASA's science mission directorate. http://www.lpi.usra.edu/vexag/road_map_final. pdf. 2006
11 Hayati S, Volpe R, Backes P, et al. The Rocky 7 rover: A Mars sciencecraft prototype. In: Proceedings of the IEEE International Conference on Robotics and Automation, Albuquerque, NM, USA: IEEE, 1997. 2458–2464
12 Zheng Y, Ouyang Z, Li C, et al. China's lunar exploration program: Present and future. Planet Space Sci, 2008, 56: 881–886
13 Maimone M, Biesiadecki J, Tunstel E, et al. Surface navigation and mobility intelligence on the Mars exploration rovers. In: Intelligence for Space Robotics. Howard A M, Tunstel E W, eds. San Antonio, TX, USA, 2006
14 Bajracharya M, Maimone M W, Helmick D. Autonomy for Mars rovers: past, present, and future. Computer, 2008, 41: 44–50
15 Maimone M W, Leger P C, Biesiadecki J J. Overview of the Mars exploration rovers' autonomous mobility and vision capabilities. In: Proceedings of the 2007 IEEE International Conference on Robotics and Automation, Space Robotics Workshop, Roma, Italy, 2007
16 Montferrer A, Bonyuet D. Cooperative robot teleoperation through virtual reality interfaces. In: Proceedings of the Sixth International Conference on Information Visualization, London, 2002. 243–248
17 Backes P G, Tharp G K, Tso K S. The Web Interface for Telescience (WITS). In: Proceedings of the IEEE International Conference on Robotics and Automation, Albuquerque, NM, USA: IEEE, 1997. 411–417
18 Wright J R, Hartman F R, Cooper B K, et al. Driving on Mars with RSVP: building safe and effective command sequences. IEEE Robot Autom Mag, 2006, 13: 37–45
19 Young K. Mars rover escapes from the "Bay of Lamentation". 2006. http://www.newscientist.com/article/dn9286-mars-rover-escapes-from-the-bay-of-lamentation.html
20 Ding L, Gao H B, Deng Z Q, et al. Design of comprehensive high-fidelity/high-speed virtual simulation system for lunar rover. In: Proc. IEEE Conference on Robotics, Automation and Mechatronics, Chengdu, China, 2008
21 Dvorak D, Bollella G, Canham T, et al. Project golden gate: towards real-time Java in space missions. In: Proceedings of the Seventh IEEE International Symposium on Object-Oriented Real-Time Distributed Computing, Vienna, Austria: IEEE, 2004. 15–22
22 JPL. Mars exploration rovers objectives. http://marsrover.nasa.gov/science/objectives.html
23 Blake D F, Morris R V, Kocurek G, et al. Curiosity at Gale Crater, Mars: Characterization and analysis of the rocknest sand shadow. Science, 2013, 341: 1239505
24 Wikipedia. Curiosity (rover). http://en.wikipedia.org/wiki/Curiosity_(rover)#cite_note-MSLUSAToday-16
25 JPL. Mars science laboratory contribution to Mars exploration program science goals. http://mars.jpl.nasa.gov/msl/mission/science/goals/
26 ESA. Scientific objectives of the ExoMars Rover. http:// exploration.esa.int/science-e/www/object/index.cfm?fobjectid=45082
27 Neal C R. The Moon 35 years after Apollo: What's left to learn? Chem Erde-Geochem, 2009, 69: 3–43
28 Tanaka S, Mitani T, Iijima Y, et al. The science objectives of Japanese Lunar Lander Project SELENE-II. In: Proceedings of the 42nd Lunar and Planetary Science Conference, The Woodlands, TX, USA, 2011
29 Harbin Institute of Technology (HIT). The Lunar Rover prototype exhibited in Zhuhai Airshow, the locomotion system of which was developed by HIT. 2006. http://today.hit.edu.cn/articles/ 2006/11-08/11132413.htm
30 Baumgartner E, Bonitz R, Melko J, et al. The Mars exploration rover instrument positioning system. In: Proceedings of the 2005 IEEE Aerospace Conference, Big Sky, MT, USA: IEEE, 2005. 1–19
31 Leger C C, Trebi-Ollennu A, Wright J R, et al. Mars Exploration Rover surface operations: driving spirit at Gusev Crater. In: Proceedings of the 2005 IEEE International Conference on Systems, Man and Cybernetics, Big Sky, MT, USA: IEEE, 2005. 1815–1822
32 JPL. MSL Science corner. http://msl-scicorner. jpl.nasa. gov/
33 Volpe R, Nesnas I, Estlin T, et al. The CLARAty architecture for robotic autonomy. In: Proceedings of the IEEE Aerospace Conference,

Big Sky, MT, USA: IEEE, 2001. 1121–1132
34 Nesnas I A D, Reid S, Danie G, et al. CLARAty: Challenges and steps toward reusable robotic software. Int J Adv Robot Syst, 2006, 3: 23–30
35 Hartman F R, Cooper B, Leger C, et al. Data visualization for effective rover sequencing. In: Proceedings of the 2005 IEEE Aerospace Conference, Big Sky, MT, USA: IEEE, 2005. 1378–1383
36 Yen J, Jain A, Balaram J. ROAMS: Rover Analysis Modeling and Simulation software. In: Proceedings of the International Symposium on Artificial Intelligence, Robotics and Automation in Space, ESTEC, Noordwijk, the Netherlands, 1999
37 Volpe R. Rover functional autonomy development for the Mars mobile science laboratory. In: Proceedings of the IEEE Aerospace Conference, Big Sky, Montana, USA: IEEE, 2003. 643–652
38 Golombek M P, Anderson R C, Barnes J R. Overview of the Mars Pathfinder mission: launch through landing, surface operations, data sheets, and science results. J Geophys Res, 1999, 104: 8523–8553
39 Richard V M, Steven W R, Ralf G, et al. Identification of Carbonate-rich outcrops on Mars by the Spirit rover. Science, 2010, 329: 421–424
40 Squyres S W, Knoll A H, Arvidson R E, et al. Two years at Meridiani Planum: Results from the Opportunity rover. Science, 2006, 313: 1403–1407
41 Herkenhoff K E, Squyres S W, Arvidson R E, et al. Evidence from Opportunity's microscopic imager for water on meridiani planum. Science, 2004, 306: 1727–1730
42 Bell III J F, Squyres S W, Arvidson R E, et al. Pancam multispectral imaging results from the Spirit Rover at Gusev Crater. Science, 2004, 305: 800–806
43 Golombek M P, Arvidson R E, Bell III J F, et al. Assessment of Mars exploration rover landing site predictions. Nature, 2005, 436: 44–48
44 Rover Team. Characterization of the Martian surface deposits by the Mars Pathfinder rover, Sojourner. Science, 1997, 278: 1765–1767
45 Fergason R L, Christensen P R, Bell III J F, et al. Physical properties of the Mars exploration rover landing sites as inferred from Mini-TES-derived thermal inertia. J Geophys Res, 2006, 111: 1–18
46 Arvidson R E, Anderson R C, Bell III J F, et al. Localization and physical properties experiments conducted by Opportunity at Meridiani Planum. Science, 2004, 306: 1730–1733
47 Arvidson R E, Anderson R C, Bartlett P, et al. Localization and physical properties experiments conducted by Spirit at Gusev Crater. Science, 2004, 305: 821–824
48 Biesiadecki J J, Baumgartner E T, Bonitz R G, et al. Mars exploration rover surface operations: Driving Opportunity at Meridiani Planum. IEEE Robot Autom Mag, 2006, 13: 63–71
49 JPL. User interfaces. http://www-robotics.jpl. nasa.gov/applications /applicationArea.cfm?App=11
50 Alami R, Chatila R, Fleury S, et al. An architecture for autonomy. Int J Robot Res, 1998, 17: 315–337
51 Estlin T, Gaines D, Bornstein B, et al. Supporting increased autonomy for a Mars rover. In: Proceedings of the International Symposium on Artificial Intelligence, Robotics and Automation in Space, Hollywood, USA, 2008
52 Ingrand F, Lacroix S, Lemai-Chenevier S, et al. Decisional autonomy of planetary rovers. J Field Robot, 2007, 24: 559–580
53 Volpe R, Nesnas I, Estlin T, et al. CLARAty: Coupled Layer Architecture for Robotic Autonomy. NASA, Jet Propulsion Laboratory, Pasadena, CA, USA, Technical Report D–19975, 2000
54 Lutz D. New Mars rover's mechanics to be used to study Martian soil properties. 2012. http://news.wustl. edu/news/pages/ 23139.aspx
55 Iagnemma K. Terrain estimation methods for enhanced autonomous rover mobility. In: Intelligence for Space Robotics. Howard A M, Tunstel E W, eds. San Antonio, TX, USA, 2006
56 Iagnemma K, Kang S, Shibly H, et al. Online terrain parameter estimation for wheeled mobile robots with application to planetary rovers. IEEE T Robot, 2004, 20: 921–927
57 Ray L E. Estimation of terrain forces and parameters for rigid-wheeled vehicles. IEEE T Robot, 2009, 25: 717–726
58 Ding L, Yoshida K, Nagatani K, et al. Parameter identification for planetary soil based on a decoupled analytical wheel-soil interaction terramechanics model. In: Proceedings of the IEEE/RSJ Int. Conf. Intelligent Robots and Systems, St. Louis, MO, USA: IEEE, 2009. 4122–4127
59 Ding L, Gao H, Deng Z, et al. An approach of identifying mechanical parameters for lunar soil based on integrated wheel-soil interaction terramechanics model of rovers (in Chinese). Acta Aeronautica Ast, 2011, 32: 1112–1123
60 Ojeda L, Cruz D, Reina G, et al. Current-based slippage detection and odometry correction for mobile robots and planetary rovers. IEEE T Robot, 2006, 22: 366–378
61 Dumond D. Terrain Classification using proprioceptive sensors. Dissertation of Doctor Degree. Hanover, NH, USA: Dartmouth College, 2011
62 Brooks C A, Iagnemma K. Vibration-based terrain classification for planetary exploration rovers. IEEE T Robot, 2005, 21: 1185–1191
63 Angelova A, Matthies L, Helmick D, et al. Learning and prediction of slip from visual information. J Field Robot, 2007, 24: 205–231
64 Leonard J J, Durrant-Whyte H F. Simultaneous map building and localization for an autonomous mobile robot. In: Proceedings of the IEEE/RSJ International Workshop on Intelligent Robots and Systems, Osaka, Japan: IEEE, 1991. 1442–1447
65 Durrant-Whyte H F, Bailey T. Simultaneous localization and mapping: Part I. IEEE Robot Autom Mag, 2006, 13: 99–110
66 Dissanayake M W M G, Newman P, Clark S, et al. A solution to the simultaneous localisation and map building (SLAM) problem. IEEE T Robotic Autom, 2006, 17: 229–241
67 Davison A J, Kita N. 3D simultaneous localization and map-building using active vision for a robot moving on undulating terrain. In: Proceedings of the 2001 IEEE Computer Society Conference on Computer Vision and Pattern Recognition, Kauai, HI, USA: IEEE, 2011
68 Davison A J. Real-time simultaneous localisation and mapping with a single camera. In: Proceedings of the Ninth IEEE International Conference on Computer Vision, Nice, France, 2003. 384–391
69 Matthies L, Maimone M, Johnson A, et al. Computer vision on Mars. Int J Comput Vision, 2007, 75: 67–92
70 Cheng Y, Maimone M W, Matthies L. Visual odometry on the Mars exploration rovers-a tool to ensure accurate driving and science imaging. IEEE Robot Autom Mag, 2006, 13: 54–62
71 Maimone M, Cheng Y, Matthies L. Two years of visual odometry on the Mars exploration rovers. J Field Robot, 2007, 24: 169–186
72 Brooks C A, Iagnemma K. Self-supervised terrain classification for planetary surface exploration rovers. J Field Robot, 2012, 29: 445–468
73 Ojeda L, Borenstein J, Witus G, et al. Terrain characterization and classification with a mobile robot. J Field Robot, 2006, 23: 103–122
74 Gennery D B. Traversability analysis and path planning for a planetary rover. Auton Robot, 1999, 6: 131–146
75 Lacroix S, Mallet A, Bonnafous D. Autonomous rover navigation on unknown terrains: functions and integration. Int J Robot Res, 2002, 21: 917–942
76 Chhaniyara S, Brunskill C, Yeomans B, et al. Terrain trafficability analysis and soil mechanical property identification for planetary rovers: a survey. J Terramechnics, 2012, 49: 115–128
77 Iagnemma K, Genot F, Dubowsky S. Rapid physics-based rough-terrain rover planning with sensor and control uncertainty. In: Proc. IEEE International Conference on Robotics and Automation, Detroit, MI, USA, 1999
78 Ishigami G, Nagatani K, Yoshida K. Path planning for planetary exploration rovers and its evaluation based on wheel slip dynamics. In: Proceedings of the IEEE International Conference on Robotics and Automation, Roma, Italy, IEEE: 2007. 2361–2366
79 Howard T M, Kelly A. Optimal rough terrain trajectory generation for wheeled mobile robots. Int J Robot Res, 2007, 26: 141–166
80 Kim J H, Kim Y H, Choi S H, et al. Evolutionary multi-objective optimization in robot soccer system for education. IEEE Comput Intell M, 2009, 4: 31–41
81 Tarokh M. Hybrid intelligent path planning for articulated rovers in rough terrain. Fuzzy Set Syst, 2008, 159: 2927–2937

82 Noguchi N, Terao H. Path planning of an agricultural mobile robot by neural network and genetic algorithm. Comput Electron Agr, 1997, 18: 187–204
83 Kolmanovsky I, McClamroch N H. Development in nonholonomic control problems. IEEE Contr Syst Mag, 1995, 15: 20–36
84 Morin P, Samson C. Control of nonholonomic mobile robots based on the transverse function approach. IEEE T Robot, 2009, 25: 1058–1073
85 Iagnemma K, Shibly H, Rzepniewski A, et al. Planning and control algorithms for enhanced rough-terrain rover mobility. In: Proceedings of the 6th International Symposium on Artificial Intelligence and Robotics & Automation in Space, St-Hubert, Quebec, Canada, 2001
86 Ishigami G, Miwa A, Nagatani K, et al. Terramechanics-based model for steering maneuver of planetary exploration rovers on loose soil. J Field Robot, 2007, 24: 233–250
87 Ding L, Gao H B, Deng Z Q, et al. Path-following control of wheeled planetary exploration robots moving on deformable rough terrain. Sci World J, 2014, http://dx.doi.org/ 10.1155/2014/ 793526
88 Helmick D M, Cheng Y, Clouse D, et al. Path following using visual odometry for a Mars rover in high-slip environments. In: Proceedings of the IEEE Aerospace Conference, Big Sky, MT, USA: IEEE, 2004. 772–789
89 Helmick D M, Roumeliotis S I, Cheng Y, et al. Slip-compensated path following for planetary exploration rovers. Adv Robotics, 2006, 20: 1257–1280
90 Ishigami G, Nagatani K, Yoshida K. Path following control with slip compensation on loose soil for exploration rover. In: Proceedings of the IEEE/RSJ International Conference on Intelligent Robots and Systems, Beijing, China: IEEE, 2006. 5552–5557
91 Ding L, Gao H B, Deng Z Q, et al. Slip-ratio-coordinated control of planetary exploration robots traversing over deformable rough terrain. In: Proceedings of the IEEE/RSJ International Conference on Intelligent Robots and Systems, Taipei, China: IEEE, 2010. 4958–4963
92 Ding L. Wheel-soil interaction terramechanics for lunar/planetary exploration rovers: Modeling and application (in Chinese). Dissertation of Doctor Degree. Harbin: Harbin Institute of Technology, Harbin, 2009
93 Xia K. Research on tracking control of mobile robot based on wheel-soil interaction modeling (in Chinese). Master dissertation, School of Mechatronics Engineering, Harbin Institute of Technology, Harbin, China, 2009
94 Wang D W, Low C B. Modeling and analysis of skidding and slipping in wheeled mobile robots: control design perspective. IEEE T Robot, 2008, 24: 676–687
95 Ding L, Gao H B, Guo J L, et al. Terramechanics-based analysis of slipping and skidding for wheeled mobile robots. In: Proceedings of the 31st Chinese Control Conference, Heifei, China: IEEE, 2012. 4966–4973
96 Ding L, Gao H B, Deng Z Q, et al. Advances in simulation of planetary wheeled mobile robots. In: Mobile Robots-Current Trends. Gacovski Z, ed. Rijeka, Croatia: In Tech Press, 2011. 375–402
97 Yen J, Jain A, Balaram J. ROAMS: Rover analysis modeling and simulation software. In: Proceedings of the International Symposium on Artificial Intelligence, Robotics and Automation in Space, ESTEC, Noordwijk, the Netherlands, 1999
98 Estlin T, Gaines D, Bornstein B, et al. Supporting increased autonomy for a Mars rover. In: Proceedings of the International Symposium on Artifcial Intelligence, Robotics and Automation in Space, Hollywood, USA, 2008
99 Zhou F, Arvidson R E, Bennett K, et al. Simulations of Mars rover traverses. J Field Robot, 2014, 31: 141–160
100 Schäfer B, Gibbesch A, Krenn R, et al. Planetary rover mobility simulation on soft and uneven terrain. Vehicle Syst Dyn, 2010, 48: 149–169
101 Ding L, Nagatani K, Sato K, et al. Terramechanics-based high-fidelity dynamics simulation for wheeled mobile robot on deformable rough terrain. In: Proceedings of the IEEE International Conference on Robotics and Automation, Anchorage, Alaska, USA: IEEE, 2010. 4922–4927
102 Wright J, Hartman F R, Cooper B, et al. Terrain modeling for immersive visualization for the Mars exploration rovers. In: Proceedings of the SpaceOps, Montreal, Canada, 2004
103 Leger P C, Deen R G, Bonitz R G. Remote image analysis for Mars exploration rover mobility and manipulation operations. In: Proceedings of the IEEE International Conference on Systems, Man and Cybernetics, Hawaii, USA, IEEE: 2005. 917–922
104 Griffiths A D, Coates A J, Jaumann R, et. al. Context for the ESA ExoMars rover: the Panoramic Camera (PanCam) instrument. Int J Astrobiol, 2006, 5: 269–275
105 Rekleitis I, Bedwani J L, Dupuis E. Autonomous planetary exploration using LiDAR data. In: Proceedings of the IEEE International Conference on Robotics and Automation, Kobe, Japan, IEEE, 2009. 3025–3030
106 Carle P J F, Furgale P T, Barfoot T D. Long-range rover localization by matching LIDAR scans to orbital elevation maps. J Field Robot, 2010, 27: 344–370
107 Yoshida K. The SpaceDyn: A MATLAB toolbox for space and mobile robots. JRM, 2000, 12: 411–416
108 Ding L, Deng Z Q, Gao H B, et al. Experimental study and analysis of the wheels' steering mechanics for planetary exploration WMRs moving on deformable terrain. Int J Robot Res, 2013, 32: 712–743
109 Bekker M G. Introduction to Terrain-Vehicle. Ann Arbor, MI, USA: The University of Michigan Press, 1969
110 Wong J Y. Terramechanics and Off-Road Vehicle Engineering. 2nd ed. Oxford, England: Elsevier, 2010
111 Ding L, Deng Z Q, Gao H B, et al. Planetary rovers' wheel–soil interaction mechanics: new challenges and applications for wheeled mobile robots. Int Serv Robot, 2011, 4: 17–38
112 Ding L, Gao H B, Deng Z Q, et al. Experimental study and analysis on driving wheels' performance for planetary exploration rovers moving in deformable soil. J Terramechnics, 2010, 48: 27–45
113 Ding L, Gao H B, Deng Z Q, et al. Wheel slip-sinkage and its prediction model of lunar rover. J Cent South Univ T, 2010, 17: 129–135
114 Ding L, Deng Z Q, Gao H B, et al. Interaction mechanics model for rigid driving wheels of planetary rovers moving on sandy terrain with consideration of multiple physical effects. J Field Robot, 2014, doi: 10.1002/rob.21533
115 Meirion-Griffith G, Spenko M. A modified pressure–sinkage model for small, rigid wheels on deformable terrains. J Terramechnics, 2011, 48: 149–155
116 Irani R A, Bauer R J, Warkentin A. A dynamic terramechanic model for small lightweight vehicles with rigid wheels and grousers operating in sandy soil. J Terramechnics, 2011, 48: 307–318
117 Gao H B, Guo J L, Ding L, et al. Longitudinal skid model for wheels of planetary exploration rovers based on terramechanics. J Terramechnics, 2013, 50: 327–343
118 Ding L, Gao H B, Deng Z Q, et al. Longitudinal slip versus skid of planetary rovers' wheels traversing on deformable slopes. In: IEEE/RSJ International Conference on Intelligent Robots and Systems, Tokyo, Japan, 2013, 2842–2848
119 Shibly H, Iagnemma K, Dubowsky S. An equivalent soil mechanics formulation for rigid wheels in deformable terrain, with application to planetary exploration rovers. J Terramechnics, 2005, 42: 1–13
120 Ding L, Gao H B, Li Y K, et al. Improved explicit-form equations for estimating dynamic wheel sinkage and compaction resistance on deformable terrain. Mech Mach Theory, 2015: 235–264
121 Guo S P, Li D X, Meng Y H, et al. Task space control of free-floating space robots using constrained adaptive RBF-NTSM. Sci China Tech Sci, 2014, 57: 828–837
122 Zhuang H C, Gao H B, Deng Z Q, et al. A review of heavy-duty legged robots. Sci China Tech Sci, 2014, 57: 298–314